www.nature.com/aps

Acta Pharmacologica Sinica

ARTICLE

Activation of mesocorticolimbic dopamine projections initiates cue-induced reinstatement of reward seeking in mice

Man-yi Jing[1], Xiao-yan Ding[1,2], Xiao Han[1], Tai-yun Zhao[1], Min-min Luo[3], Ning Wu[1], Jin Li[1] and Rui Song[1]

Drug addiction is characterized by relapse when addicts are re-exposed to drug-associated environmental cues, but the neural mechanisms underlying cue-induced relapse are unclear. In the present study we investigated the role of a specific dopaminergic (DA) pathway from ventral tegmental area (VTA) to nucleus accumbens core (NAcore) in mouse cue-induced relapse. Optical intracranial self-stimulation (oICSS) was established in DAT-Cre transgenic mice. We showed that optogenetic excitation of DA neurons in the VTA or their projection terminals in NAcore, NAshell or infralimbic prefrontal cortex (PFC-IL) was rewarding. Furthermore, activation of the VTA-NAcore pathway alone was sufficient and necessary to induce reinstatement of oICSS. In cocaine self-administration model, cocaine-associated cues activated VTA DA neurons as assessed by intracellular GCaMP signals. Cue-induced reinstatement of cocaine-seeking was triggered by optogenetic stimulation of the VTA-NAcore pathway, and inhibited by chemogenetic inhibition of this pathway. Together, these results demonstrate that cue-induced reinstatement of reward seeking is in part mediated by activation of the VTA-NAcore DA pathway.

Keywords: drug addiction; dopamine; ventral tegmental area; nucleus accumbens; medial prefrontal cortex; optogenetic; optical intracranial self-stimulation; cocaine self-administration

Acta Pharmacologica Sinica (2022) 43:2276–2288; https://doi.org/10.1038/s41401-022-00866-x

INTRODUCTION

Drug addiction is characterized by high rates of relapse when drug users are re-exposed to addictive drugs, environmental cues associated with drug use, or stress [1–3]. In humans, relapse triggered by drug-associated cues is the most common and the major reason that success in maintaining abstinence is impeded [4–6]. Thus, understanding the neural mechanisms underlying cue-induced relapse is critical to develop effective treatment strategies to promote drug abstinence.

The development of drug addiction is believed to derive from maladaptive neurobiological responses to drugs of abuse in the mesocorticolimbic dopamine (DA) systems and the corticostriatal glutamate projection systems [7, 8]. Evidence has shown that relapse triggered by drugs is largely DA-dependent since most addictive drugs increase extracellular DA in the nucleus accumbens (NAc) by different cellular and molecular mechanisms [9–11]. However, little is known about the role of DA in cue-induced relapse. Evidence has shown that the blockade of DA D1 or D2 receptors in the NAc attenuates cue-evoked cocaine or heroin seeking [12, 13], and the activation of D2 receptor-expressing medium-spiny neurons (MSNs) or increased DA release in the NAc is associated with increased motivation to seek drugs [14]. In contrast, there is also evidence indicating that increased DA efflux in the PFC, but not in the NAc, is associated with conditioned stimulus (cue)-induced reinstatement of methamphetamine seeking [15], and increased DA release in the NAcore may suppress glutamatergic plasticity and cue-induced drug seeking [16]. Alternatively, transient potentiation of glutamate transmission in the NAc, indicated by increases in the ratio of AMPA to NMDA currents and dendritic spine head diameter and density at glutamatergic synapses [17–19], has been shown to be involved in cue-induced reinstatement of drug-seeking behavior [20–23]. The reasons for the conflicting findings regarding DA are unknown, which may be related to the obvious limits of classic experimental approaches, such as in vivo brain microdialysis, which has poor temporal and spatial resolution, and intracranial drug microinjections and pharmacological manipulations, which lack cell type specificity [24–26].

Optogenetic and chemogenetic techniques have allowed us to precisely manipulate specific neuron types to observe their role in motivated behavior at extremely high temporal and spatial resolution. Using these new cutting-edge techniques, it has been shown that phasic firing in midbrain DA neurons is critically involved in normal Pavlovian learning and cue-conditioned reward [27–29]. However, it is unknown whether brief firing in DA neurons is also required in cue-induced reinstatement (relapse) of reward-seeking behavior. The mesocorticolimbic DA system is composed of anatomically and functionally heterogeneous DA subpopulations that project to different brain regions, such as the shell and core of the NAc, dorsal striatum, and prelimbic and infralimbic prefrontal cortex [30]. In this study, we used new techniques to dissect the role of each DA projection pathway in cue-induced reinstatement. We first used optogenetic intracranial self-stimulation

[1]State Key Laboratory of Toxicology and Medical Countermeasures, Beijing Key Laboratory of Neuropsychopharmacology, Beijing Institute of Pharmacology and Toxicology, Beijing 100850, China; [2]Nanjing University of Chinese Medicine, Nanjing 210029, China and [3]National Institute of Biological Sciences, Beijing 102206, China
Correspondence: Ning Wu (wuning7671@126.com) or Jin Li (jinli9802@163.com) or Rui Song (songrui1983@yeah.net)
These authors contributed equally: Man-yi Jing, Xiao-yan Ding

Received: 9 August 2021 Accepted: 13 January 2022
Published online: 25 February 2022

(oICSS) to study whether the stimulation of VTA DA neurons or their projection terminals in different brain regions is rewarding and whether oICSS-associated cues (lights) can evoke the reinstatement of oICSS maintained by the stimulation of different DA pathways in DAT-Cre mice. We then observed whether re-exposure to cocaine-associated cues activates VTA DA neurons by recording intracellular Ca^{2+} signal fluctuations during cue-induced reinstatement. Finally, we observed whether optogenetic or chemogenetic manipulation of distinct DA projection pathways alters cue-induced cocaine reinstatement. We found that the VTA-NAcore DA pathway, but not the other pathways, plays an essential role in cue-induced reinstatement of reward-seeking behavior.

MATERIALS AND METHODS

Animals

All experiments were performed with male adult DAT-Cre BAC transgenic mice (strain B6.SJL-Slc6a3tm1.1 (cre) Bkmn/J, Jackson Laboratory, Bar Harbor, ME, USA). DAT-Cre mice, 8–15 weeks old, were housed individually in a temperature- and humidity-controlled environment (22 °C, 50%–60% humidity, 12/12-h light/dark cycle with lights on at 8:00 a.m. and lights off at 8:00 p.m.) and provided with food and water *ad libitum*. Littermates were assigned to experimental and control groups whenever possible. Experiments were all conducted during the animal's light cycle. Animal experiments were performed in accordance with the NIH guidelines for the Care and Use of Laboratory Animals. All experimental procedures were approved by the Institutional Review Committee (IACUC-DWZX-2021-750).

Viruses

rAAV-EF1α-DIO-hChR2-mCherry-WPRE-pA (serotypes: AAV2/9, titers: 5.27×10^{12} μg/mL, volume: 500 nL), rAAV-EF1α-DIO-hM4Di-YFP-WPRE-pA (serotypes: AAV2/9, titers: 5.27×10^{12} μg/mL, volume: 500 nL) and rAAV-EF1α-DIO-GCaMP6m-WPRE-pA (serotypes: AAV2/9, titers: 5.27×10^{12} μg/mL, volume: 500 nL) were all purchased from BrainVTA Co., Ltd. (Wuhan, China).

Drugs

Cocaine was provided by Beijing Public Security Bureau Forensic Medical Examination Center (Beijing, China) and freshly dissolved in 0.9% saline to obtain the indicated doses (0.5 mg/kg per injection). Clozapine nitrogen oxide (CNO, Sigma–Aldrich LLC., St. Louis, USA) was dissolved in 0.036% DMSO to obtain the indicated doses (0.03 μg/kg per side) [31].

Apparatus

The laser-induced self-stimulation experiments were conducted in operant test chambers (200 mm × 150 mm × 180 mm, L × W × H). Each test chamber had two nose-poke holes (Aes-110, ID = 2 cm) located 4.5 cm above the floor (Anilab SuperState Version 4.0, Anilab Software & Instruments Co., Ltd., Ningbo, China). Anilab 6.53 software was applied to schedule the experimental events and collect the data.

The fiber photometry system was produced by Thinker Tech Nanjing Biotech Limited Co. (Nanjing, China). To record fluorescence signals, 470-nm excitation light was reflected by a dichroic mirror (MD498; Thorlabs, Inc., New Jersey, USA) and focused by a 20 × 0.4 objective. An optical fiber (230 mm O.D., numerical aperture (NA) = 0.37, 2 m long) guided the light between the objective and the implanted optical fiber. The GCaMP fluorescence was bandpass filtered (MF525-39; Thorlabs, Inc., New Jersey, USA) and collected by a photomultiplier tube (H10721-210; Hamamatsu Photonics, Hamamatsu, Japan). An amplifier was used to convert the photomultiplier tube current output to voltage signals, which were further filtered through a 40-Hz low-pass filter.

Virus injection and implantation

Animals were anesthetized with sodium pentobarbital (70 mg/kg, i.p.). Animals were then placed in a stereotaxic device (RWD Life Science, Shenzhen, China) for virus injection and optical fiber insertion. For VTA manipulation experiments, rAAV constructs were injected unilaterally into the VTA at the following coordinates relative to bregma: AP −3.2 mm, ML −0.5 mm, and DV −3.7 mm (DV measured from the dura surface). The injection was performed with a WPI Nanoliter 2000 injector (WPI, Florida, USA) at a rate of 43 nL/min. The injector remained in place for an additional 10 min. Subsequently, a single optic fiber cannula (Cat. No. 62003, 480 μm × 340 μm, O.D. × I.D.; RWD Life Science, Shenzhen, China) was implanted unilaterally above the VTA at the following coordinates relative to bregma: AP −3.2 mm, ML −0.5 mm, and DV −3.7 mm (DV measured from the dura surface). Fiber cannulas were secured using instant adhesive (Cat. No. 145401, TONSAN, Beijing, China) followed by the application of acrylic dental cement. Animals recovered for 2 weeks postsurgery. To stimulate the NAcore, NAshell, IL-PFC or PL-PFC in DAT-Cre^{+} mice, fiber cannulas were placed ipsilaterally above the NAcore, NAshell, IL-PFC and PL-mPFC, respectively, following unilateral virus injection into the VTA. The fiber cannula coordinates were as follows: AP + 1.6 mm, ML + 0.8 mm, and DV −4.1 mm (DV measured from the skull) for the NAcore; AP + 1.6 mm, ML + 0.8 mm, and DV −4.35 mm (DV measured from the skull) for the NAshell; AP + 1.6 mm, ML + 0.4 mm, and DV −1.9 mm (DV measured from the dura) for the IL-mPFC; and AP + 1.6 mm, ML + 0.4 mm, and DV −1.2 mm (DV measured from the dura) for the PL-mPFC. On the other hand, to silence DA projections through chemogenetic techniques in the NAcore, NAshell, IL-PFC and PL-PFC, CNO-injected cannulas were bilaterally placed above the NAcore, NAshell, IL-PFC and PL-PFC, respectively, following bilateral virus (rAAV-EF1α-DIO-hM4Di-YFP-WPRE-pA, 500 nL/side) injection into the VTA at the following coordinates: AP −3.2 mm, ML ± 0.5 mm, and DV −4.2 mm (DV measured from the dura). Then, the cannulas at these terminals were implanted using the following coordinates: AP + 1.6 mm, ML ± 2.5 mm, and DV −4.4 mm (DV measured from the skull) for the NAcore; AP + 1.6 mm, ML ± 2.55 mm, and DV −4.66 mm (DV measured from the skull) for the NAshell; AP + 1.6 mm, ML ± 1.27 mm, and DV −2.05 mm (DV measured from the dura) for the IL-PFC; and AP + 1.6 mm, ML ± 1.02 mm, and DV −1.31 mm (DV measured from the dura) for the PL-PFC with coordinates at a 20 degree angle. To record the activity of DA neurons in the VTA in the fiber photometry experiments, rAAV-EF1α-DIO-GCaMP6m-WPRE-pA virus was microinjected into the VTA (AP −3.2 mm, ML −0.5 mm, and DV −4.2 mm (from the dura)) unilaterally following the above description. Subsequently, a single optic fiber (230 μm O.D., NA = 0.37; Shanghai Fiblaser, Shanghai, China) was implanted unilaterally above the VTA. The stereotaxic surgeries were performed according to the mouse brain stereotaxic atlas of Franklin and Paxinos (2007). The representation of the location of the cannula or optical fiber is shown in Supplementary Fig. S2. All locations of implantation in every experiment are schematically shown in Supplementary Figs. S3–S8.

Fiber optic implants for in vivo optogenetics were custom made from a 200 μm core/0.37 NA/230 μm outer diameter optic fiber (FC/PC-W200(PI)-2-Weixian; Beijing Viasho Technology Co., Ltd., Beijing, China). Blue light was produced with a 473-nm diode pump solid-state (DPSS) laser (VA-I-N-473; Beijing Viasho Technology Co., Ltd., Beijing, China). The laser power was adjusted to 20 mW at the exit of the implant tip for each animal.

Optical intracranial self-stimulation (oICSS) experiments

The laser-induced self-stimulation experiments were conducted in an operant test chamber. The oICSS procedure in DAT-Cre mice was carried out as previously described with minor revisions [32]. Each daily training session lasted for 60 min. The training was performed for 10–12 sessions. After establishing optical self-stimulation, the mice underwent extinction training. During extinction, the active pokes and

inactive pokes had no consequences, and the laser-stimulation-associated cue light was turned off. Daily 1-h extinction sessions for each mouse continued until pokes showed <10% variability for at least 3 consecutive days.

oICSS-associated cues reinstate extinguished oICSS behavior. Five groups of mice expressing ChR2-mCherry, the VTA ($n = 6$), NAcore ($n = 5$), NAshell ($n = 10$), IL ($n = 9$) and PL ($n = 6$) groups, were stimulated to establish VTA-oICSS, NAcore-oICSS, NAshell-oICSS, IL-oICSS and PL-oICSS, respectively. After extinction, the cue was used to challenge the mice. The numbers of active and inactive pokes were recorded before and after cue-induced reinstatement.

Optogenetic activation of the VTA-NAcore pathway triggers the reinstatement of reward-seeking behavior. Four groups of mice expressing ChR2-mCherry, the NAcore ($n = 7$), NAshell ($n = 7$), IL ($n = 4$) and PL ($n = 4$) groups, were stimulated with VTA DA neurons to establish VTA-oICSS. After extinction, the DA projections were stimulated with 100 laser stimulations (LSs) at 20 or 80 Hz into the projection targets (NAcore, NAshell, IL and PL) via optic fibers to induce reinstatement. The numbers of active and inactive pokes were recorded before and after reinstatement.

Chemogenetic inhibition of the VTA-NAcore pathway blocks cue-induced reinstatement of VTA-oICSS behavior. Mice ($n = 7$) expressing ChR2-mCherry and hM4Di-YFP were stimulated with VTA DA neurons to establish VTA-oICSS. After extinction, mice were randomly chosen to receive CNO (0.9 ng/0.5 μL per side) or vehicle bilaterally into the NAcore to inhibit VTA-NAcore projections. Then, the cue was used to challenge the mice. The numbers of active and inactive pokes were recorded before and after cue-induced reinstatement.

The VTA-NAcore DA projection pathway independently initiates reinstatement. Three groups of mice expressing ChR2-mCherry, the NAcore ($n = 8$), NAshell ($n = 10$) and IL ($n = 9$) groups, were stimulated to establish NAcore-oICSS, NAshell-oICSS and IL-oICSS, respectively. After extinction, DA projections were stimulated with 150 laser stimulations (LSs) at 80 Hz into the projection targets (NAcore, NAshell and IL) to induce reinstatement tests in the same self-stimulation chambers. The numbers of active and inactive pokes were recorded before and after reinstatement.

Intravenous cocaine self-administration

Intravenous catheterization surgery was carried out as we have reported previously [33]. Briefly, after recovery from surgery, the mice were trained to self-administer cocaine in the operant test chamber on an FR1 reinforcement schedule. Active pokes, but not inactive pokes, resulted in an injection of cocaine (0.5 mg/kg per infusion; infusion pump delivered 0.015 mL over 0.75 s) and exposure to the 5-s cue light. Then, there was a 4.25-s timeout period. We set a maximal number of 50 infusions during each 2-h session at this initial drug dose to prevent cocaine overdose. Stable self-administration was defined as <10% variability in the number of active responses for at least 3 consecutive days. When cocaine self-administration was established as described above, the experimental animals underwent extinction training. In the reinstatement test, cue-induced cocaine-seeking behavior was assessed under FR1 conditions when the cocaine-associated cue light was presented following each nose poke. However, the cocaine infusion was replaced with saline.

Cocaine-associated cues activate VTA DA neurons during reinstatement. To record the activity of DA neurons in the VTA during the cue-induced reinstatement session, mice expressing GCaMP6m ($n = 5$) were recorded with the fiber photometry system, and the Ca^{2+} signals of VTA DA neurons in the freely moving mice were collected at a sampling frequency of 100 Hz. The intensity of the excitation light at the distal end of the optical fiber was adjusted to 40 μW. The signals were recorded every day as a control during the last 5 extinction sessions. In the cue-induced reinstatement session, the Ca^{2+} signals of VTA DA neurons were also collected when cue-induced cocaine-seeking behavior occurred. Each reinstatement test lasted for 2 h.

Chemogenetic inhibition of DA transmission in the NAcore blocks cue-induced reinstatement of cocaine-seeking behavior. Four groups of mice expressing hM4Di-YFP, the NAcore ($n = 8$), NAshell ($n = 4$), IL ($n = 3$) and PL ($n = 4$) groups, were trained to self-administer cocaine. After extinction, mice were randomly chosen to receive CNO (0.9 ng/0.5 μL per side) or vehicle bilaterally into the NAcore, NAshell, IL or PL 10 min prior to the test session. Then, the mice were placed into the same chambers and exposed to cue-induced relapse.

Optogenetic activation of DA release in the NAcore triggers cue-induced cocaine-seeking behavior. Four groups of mice expressing ChR2-mCherry, the NAcore ($n = 9$), NAshell ($n = 7$), IL ($n = 7$) and PL ($n = 8$) groups, were trained to self-administer cocaine. After extinction, the DA projections were stimulated with 100 laser stimulations (LSs) at 20 or 80 Hz into the projection targets (NAcore, NAshell, IL and PL) via optic fibers to induce reinstatement. The numbers of active and inactive pokes were recorded before and after reinstatement.

Immunofluorescence

To confirm ChR2 expression on DA neurons, DAT-Cre mice injected with ChR2-mCherry were anesthetized to detect the colocalization of mCherry and tyrosine hydroxylase (TH) in the VTA, NAc and mPFC. Brain sections containing the VTA, NAc or mPFC were incubated with rabbit anti-TH monoclonal antibody (1:500; ab6211; Abcam, Boston, USA) and further incubated with a secondary antibody, goat anti-rabbit Alexa Fluor 488 IgG for TH (1:200; ZF-0511; ZSGB-BIO, Beijing, China). Fluorescent images were obtained with confocal microscopy (Olympus, Tokyo, Japan).

To confirm GCaMP6m expression on DA neurons, the colocalization of GCaMP6m and TH in the VTA was detected in DAT-Cre mice. Immunofluorescence experiments were then performed using a rabbit anti-TH monoclonal antibody (1:500; ab6211; Abcam, Boston, USA) and a secondary antibody, goat anti-rabbit Alexa Fluor 594 IgG for TH (1:200; ZF-0516; ZSGB-BIO, Beijing, China). Fluorescent images were obtained with confocal microscopy (Olympus, Tokyo, Japan).

DAT-Cre mice for the cocaine self-administration experiments were injected with ChR2-mCherry unilaterally or hM4Di-YFP bilaterally in the VTA. Thus, we detected the colocalization of TH and ChR2 and TH and hM4Di in the VTA. The preparation of brain sections was described above. Fluorescent images were obtained with confocal microscopy (Olympus, Tokyo, Japan).

Data analysis and statistical tests

All data are presented as the mean ± SEM and analyzed by SigmaState 3.5. One-way repeated measures analysis of variance (RM ANOVA) was used to analyze the number of active pokes or inactive pokes during extinction and reinstatement in all experiments (the values for extinction are represented by the average number of active pokes or inactive pokes in the last 3 consecutive sessions). The accepted level of significance for all tests was $P < 0.05$.

Photometry data were exported to MATLAB files for further analysis. After smoothing the data with a moving average filter (10-ms span), we segmented the data based on behavioral events within individual trials. We derived fluorescence change ($\Delta F/F$) values by calculating $(F\text{-}F_0)/F_0$, where F0 is the baseline fluorescence signal averaged over a 1.5-s control time window, which was typically set at 0.5 s before the cue. $\Delta F/F$ values are

presented with heatmaps and average plots with shaded areas indicating SEMs.

To quantitatively distinguish VTA DA neuron activity between extinction and reinstatement induced by cues, the mean values of $\Delta F/F$ over 0–5 s (cue present in reinstatement) were assessed by paired *t* tests. The accepted level of significance was $P < 0.05$.

RESULTS

Stimulation of VTA DA neurons or their projection terminals is rewarding

To determine the role of the mesocorticolimbic DA system in cue-induced reinstatement of reward seeking, we first examined whether optical stimulation of VTA DA neurons or their distinct projection terminals is rewarding. Figure 1 shows the general experimental methods and the results. DAT-Cre mice received intra-VTA microinjection of the AAV-ChR2 vector to express ChR2-mCherry in VTA DA neurons, which project to multiple brain regions, including the NAc and mPFC (Fig. 1a). According to the active-poke response for different frequencies of VTA-oICSS, ChR2 could be regulated well by laser stimulation (0–100 Hz) (Supplementary Fig. S1c). We selected 20 Hz, which is closer to the phasic firing of DA neurons, to establish oICSS. The ratio of TH and mCherry colocation is shown in Supplementary Fig. S3a. The parameters of laser stimulation are shown in Fig. 1b. Notably, optical stimulation of each brain region produced robust oICSS responses (black bars in Fig. 1c–f). The response caused by laser stimulation of VTA DA neurons was the most potent (Fig. 1c, ~500 pokes per hour), while the response maintained by the stimulation of the PFC-PL was the weakest (Fig. 1g, ~30 pokes per hour). Therefore, the PFC-PL region was removed in the following experiments. In contrast, the numbers of active and inactive nose pokes of mice were not significantly different before laser stimulation, as shown in Supplementary Fig. S1a, b. The locations of implantation in the VTA, NAc and mPFC are schematically shown in Supplementary Fig. S3b-f. To detect DA release when VTA DA neurons were activated chemogenetically, a DA neurotransmitter probe was used to monitor the dynamics of DA in the NAc through fiber photometry. CNO treatment increased DA release in the NAc compared to vehicle (2% DMSO) treatment in mice expressing hM3Dq ($P = 0.001$) (Supplementary Fig. S9). The results showed that the activation of DA neurons in the VTA induced drastic DA release in the NAc. These findings suggested that the activation of VTA DA neurons or their projection areas in the NAshell, NAcore or PFC-lL is rewarding, consistent with our anatomic findings that high densities of ChR2-mCherry expression were detected in these brain regions after intra-VTA AAV-ChR2-mCherry microinjections (Fig. 1a).

oICSS-associated cues reinstate extinguished oICSS behavior

After the acquisition of stable oICSS, mice underwent extinction sessions in the same context until reward-seeking behavior (nose poke responding) was extinguished. We found that re-exposure to oICSS-associated cues reinstated active nose-poke responses in mice after the extinction of the previous oICSS of VTA DA neurons (Fig. 1c, active poke: one-way RM ANOVA: cue priming main effect: $F_{(1,5)} = 14.414$, $P = 0.013$; inactive poke: one-way RM ANOVA: cue priming main effect: $F_{(1,5)} = 1.010$, $P = 0.361$). Similar cue-induced reinstatement responses were also observed in mice after the extinction of the oICSS of DA terminals in the NAcore (Fig. 1d, active poke: one-way RM ANOVA: cue priming main effect: $F_{(1,4)} = 64.306$, $P = 0.001$; inactive poke: one-way RM ANOVA: cue priming main effect: $F_{(1,4)} = 1.104$, $P = 0.353$), in the NAshell (Fig. 1e, active poke: one-way RM ANOVA: cue priming main effect: $F_{(1,9)} = 14.731$, $P = 0.004$; inactive poke: one-way RM ANOVA: cue priming main effect: $F_{(1,9)} = 1.055$, $P = 0.331$), and in the mPFC-lL (Fig. 1f, active poke: one-way RM ANOVA: cue priming main effect: $F_{(1,8)} = 56.760$, $P < 0.001$; inactive poke: one-way RM ANOVA: cue priming main effect: $F_{(1,8)} = 0.406$, $P = 0.542$). *Post hoc* individual group comparisons by Bonferroni tests revealed a significant increase in active pokes with cue-induced reinstatement compared to that with extinction, without a change in the number of inactive pokes. These results indicated for the first time that brief phasic activation of either VTA DA neurons or their projection terminals in the NAc, NAshell or mPFC-lL was sufficient to establish cue-induced oICSS.

Optogenetic activation of the VTA-NAcore pathway triggers the reinstatement of reward-seeking behavior

To determine which DA projection pathway is essential in cue-induced reinstatement, we observed reinstatement responses to the brief phasic stimulation (laser priming) of DA terminals in different brain regions in DAT-Cre mice after the extinction of oICSS of VTA DA neurons. We found that laser priming stimulation of the NAcore induced significant reinstatement of oICSS (Fig. 2a), active poke: one-way RM ANOVA: laser priming main effect: $F_{(1,6)} = 9.755$, $P = 0.02$; inactive poke: one-way RM ANOVA: laser priming main effect: $F_{(1,6)} = 0.470$, $P = 0.519$. *Post hoc* individual group comparisons assessed by Bonferroni tests revealed a significant increase in the number of active pokes during laser-induced reinstatement compared to those during extinction, without a change in the number of inactive pokes, while the stimulation of other DA projection terminals in the NAshell (Fig. 2b, active poke: one-way RM ANOVA: laser priming main effect: $F_{(3,18)} = 0.689$, $P = 0.571$; inactive poke: one-way RM ANOVA: laser priming main effect: $F_{(3,18)} = 1.171$, $P = 0.348$), in the mPFC-IL (Fig. 2c, active poke: one-way RM ANOVA: laser priming main effect: $F_{(3,9)} = 0.114$, $P = 0.950$; inactive poke: one-way RM ANOVA: laser priming main effect: $F_{(3,9)} = 3.808$, $P = 0.052$), or in the mPFC-PL (Fig. 2d, active poke: one-way RM ANOVA: laser priming main effect: $F_{(3,9)} = 0.411$, $P = 0.749$; inactive poke: one-way RM ANOVA: laser priming main effect: $F_{(3,9)} = 0.245$, $P = 0.863$) did not induce the reinstatement of oICSS. The locations of implantation in the VTA, NAc and mPFC are schematically shown in Supplementary Fig. S4a–d. These results suggested that the activation of the VTA-NAcore DA pathway alone was sufficient to trigger the reinstatement of reward-seeking behavior.

Chemogenetic inhibition of the VTA-NAcore pathway blocks cue-induced reinstatement of VTA-oICSS behavior

To confirm the above finding, we further observed the effects of chemogenetic inhibition of the VTA-NAcore pathway on cue-induced reinstatement of oICSS in DAT-Cre mice with intra-VTA AAV-ChR2 microinjections. Figure 2e shows the expression of ChR2-mCherry (red) and hM4Di-YFP (green) in the VTA and NAcore. The percentage of TH and hM4di colocation is shown in Supplementary Fig. S4e. High densities of hM4Di were detected in the NAcore. After the extinction of the oICSS of VTA DA neurons, the mice were challenged with cue light priming. Before cue priming, vehicle or clozapine nitrogen oxide (CNO) (0.9 ng) was microinjected into the NAcore of randomly chosen mice (Fig. 2f). When the mice were injected with vehicle, the cue induced significant reinstatement of the oICSS of VTA DA neurons (Fig. 2g). This response was blocked by the microinjection of CNO into the NAcore (Fig. 2g, active pokes: one-way RM ANOVA: treatment main effect: $F_{(3,18)} = 13.024$, $P < 0.001$; inactive pokes: one-way RM ANOVA: treatment main effect: $F_{(3,9)} = 1.817$, $P = 0.180$). *Post hoc* individual group comparisons revealed a significant increase in cue-induced reinstatement in the vehicle-treated mice but not in the CNO-treated mice. The location of implantation in the NAcore is schematically shown in Supplementary Fig. S4f. These results demonstrated that VTA-NAcore DA projections were necessary for cue-induced reinstatement of oICSS.

The VTA-NAcore DA projection pathway independently initiates reinstatement

Based on the above findings, an important question arose: were the DA projections to the NAcore innervated by other neural circuits or

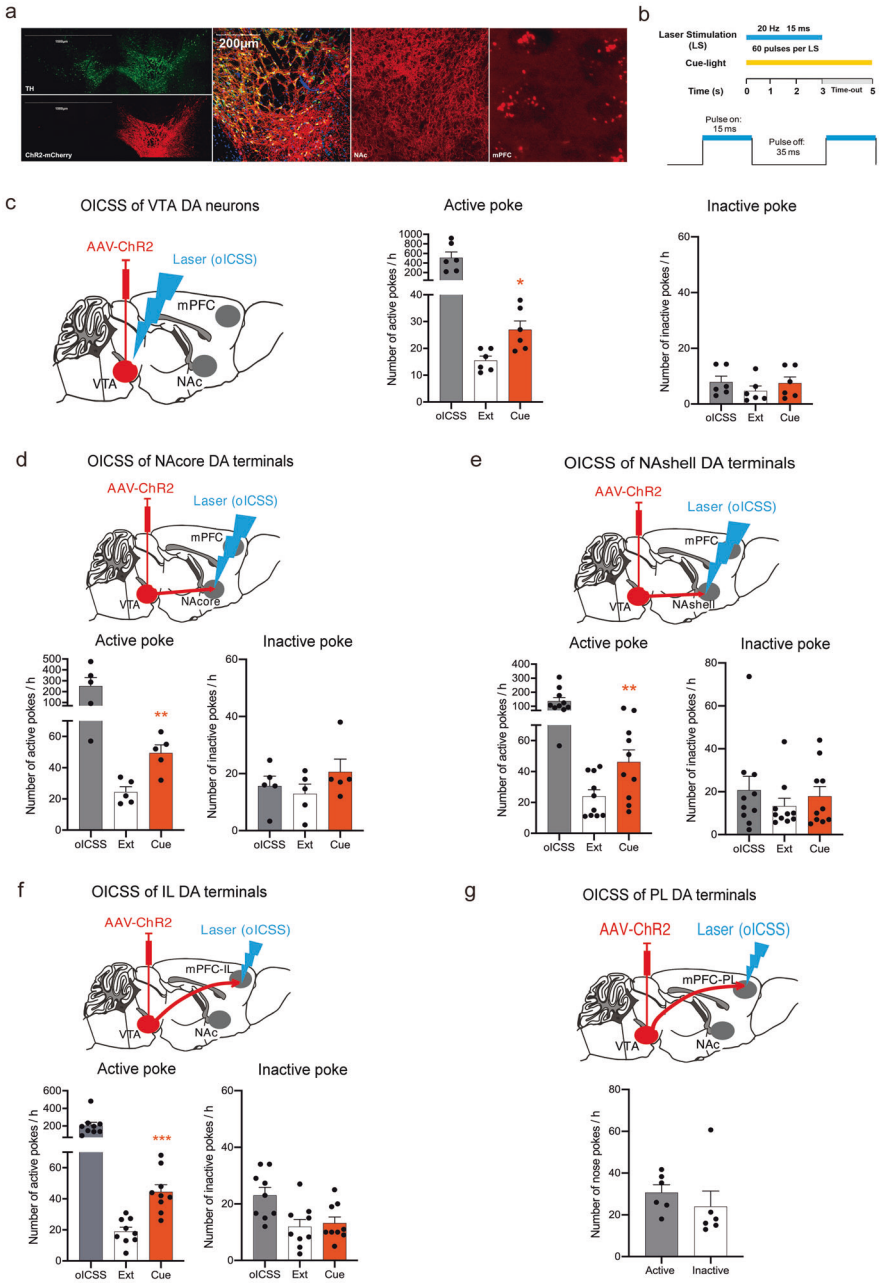

Fig. 1 Brain-stimulation reward-associated cue lights reinstate optical intracranial self-stimulation (oICSS) behavior. a Representative images illustrating ChR2-mCherry expression in the VTA, NAc and mPFC in DAT-Cre mice after intra-VTA AAV-ChR2 microinjection. 10×, scale bar = 1500 μm; 20×, scale bar = 200 μm. **b** Schematics of laser stimulation: one active nose poke resulted in the delivery of a 3-s laser stimulation and a 5-s cue light, while inactive pokes had no consequences. The pulse was a 20-Hz 473 nm blue laser with a 15-ms pulse duration. **c** Mean numbers of nose pokes in active and inactive holes during the last 3 sessions of the acquisition, the last 3 sessions of extinction, and the cue reinstatement test. oICSS-associated cue lights reinstated active-poke responses after the extinction of oICSS. One-way RM ANOVA revealed a cue priming main effect: $F_{(1,5)} = 14.414$, $P = 0.013$. *Post hoc* Bonferroni tests revealed statistically significant differences in cue-induced active-poke responses ($^{*}P < 0.05$, compared to the mean of the last 3 sessions of extinction, $n = 6$). **d** Cue-induced reinstatement of oICSS in mice with intra-VTA AAV-ChR2 microinjection but with optical fiber implantation into the NAcore for oICSS. One-way RM ANOVA: cue priming main effect: $F_{(1,4)} = 64.306$, $P = 0.001$. *Post hoc* Bonferroni tests indicated significant differences in cue-induced active-poke responses ($^{**}P < 0.01$, compared to the mean of last 3 sessions of extinction, $n = 5$). **e** Cue-induced reinstatement of oICSS in mice with intra-NAshell fiber implantation for oICSS. One-way RM ANOVA: cue priming main effect: $F_{(1,9)} = 14.731$, $P = 0.004$. *Post hoc* Bonferroni tests indicated significant differences in cue-induced active nose-poke responses ($^{**}P < 0.01$, compared to extinction, $n = 10$). **f** Cue-induced reinstatement of oICSS in mice with intra-mPFC-IL fiber implantation for oICSS. One-way RM ANOVA: cue priming main effect: $F_{(1,8)} = 56.760$, $P < 0.001$. *Post hoc* Bonferroni tests indicated significant differences in cue-induced reinstatement responses ($^{***}P < 0.001$, compared to extinction, $n = 9$). **g** Mice with intra-VTA AAV microinjection and intra-mPFC-PL fiber implantation did not acquire oICSS ($n = 6$).

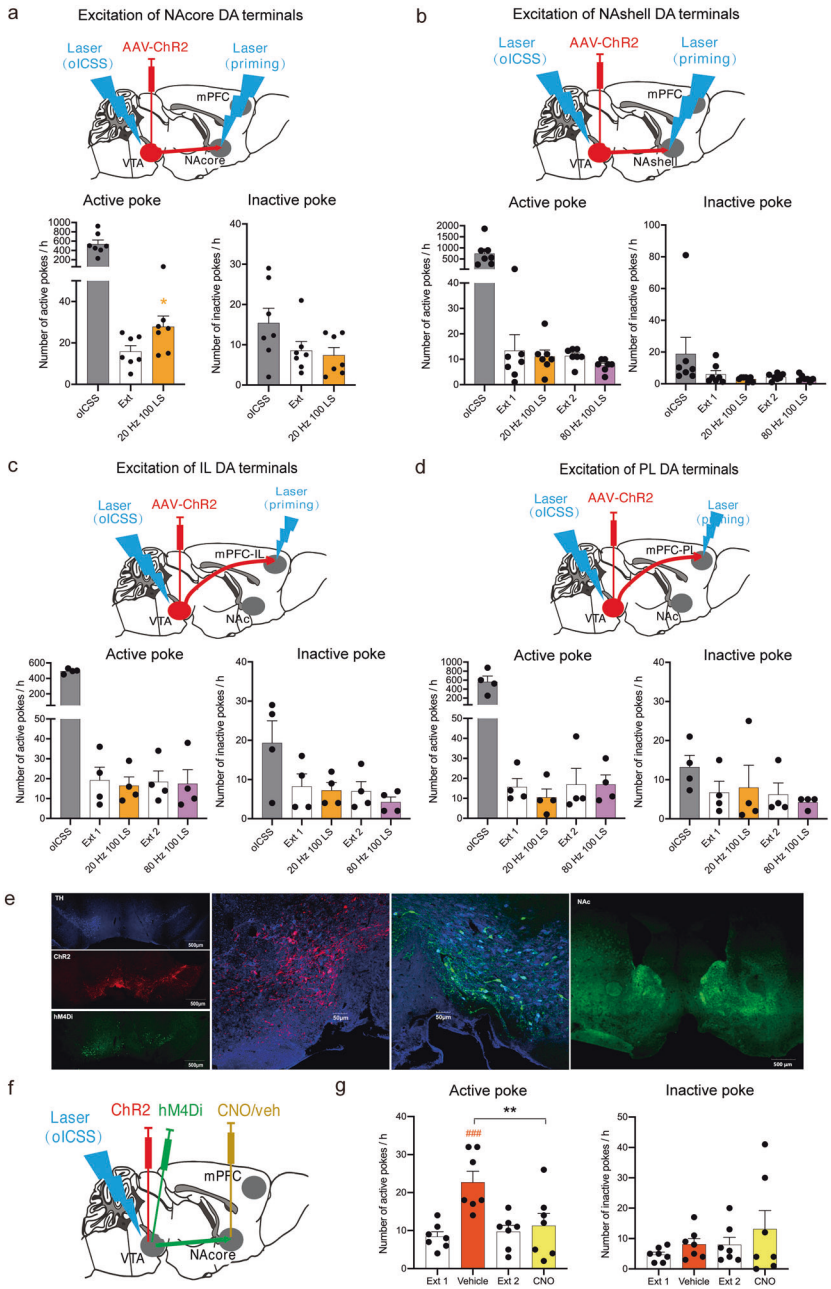

Fig. 2 VTA-NAcore DA projection pathway selectively regulates cue-induced brain-stimulation reward. a Mean numbers of nose pokes in active and inactive holes during the last 3 sessions of oICSS of VTA DA neurons, the last 3 sessions of extinction, and the laser-induced reinstatement test. The activation of the VTA-NAcore DA projections (20-Hz, 100 LS) reinstated active-poke responses in mice after the extinction of previous oICSS. One-way RM ANOVA revealed a laser priming main effect: $F_{(1,6)} = 9.755$, $P = 0.020$. *Post hoc* Bonferroni tests revealed that activation of the VTA-NAcore DA projections resulted in statistically significant differences in reinstated active-poke responses ($^{*}P < 0.05$, compared to the mean of last 3 sessions of extinction, $n = 7$). **b** Activation of DA projections to the NAshell did not reinstate active-poke responses in mice after the extinction of oICSS. One-way RM ANOVA revealed a laser priming main effect: $F_{(3,18)} = 0.689$, $P = 0.571$, $n = 7$. **c** Activation of DA projections to the IL did not reinstate active-poke responses in mice after the extinction of oICSS. One-way RM ANOVA revealed a laser priming main effect: $F_{(3,9)} = 0.114$, $P = 0.950$, $n = 4$. **d** Activation of the VTA-PL DA projections did not reinstate active-poke responses in mice after the extinction of oICSS. One-way RM ANOVA revealed a laser priming main effect: $F_{(3,9)} = 0.411$, $P = 0.749$, $n = 4$. **e** Representative images illustrating ChR2-mCherry and hM4Di-YFP expression in the VTA and hM4Di-YFP expression in the NAc of DAT-Cre mice after intra-VTA AAV-ChR2 and AAV-hM4Di microinjections. 10×, scale bar = 500 μm; 20×, scale bar = 50 μm. **f** Diagram of the conducted experiment. **g** Microinjection of CNO into the NAcore significantly decreased the cue-induced active-poke responses in mice after the extinction of oICSS. One-way RM ANOVA revealed a treatment main effect: $F_{(3,18)} = 13.024$, $P < 0.001$. The *post hoc* Holm-Sidak test revealed that the difference in cue-induced active-poke responses was statistically significant ($^{\#\#\#}P < 0.001$, compared to the mean of the last 3 sessions of Ext 1), and the difference in cue-induced active-poke responses during CNO or vehicle microinjection was significantly different ($^{**}P < 0.01$, compared to vehicle, $n = 7$). Inactive pokes were not affected by cue light or microinjection after the extinction of oICSS. One-way RM ANOVA: treatment main effect: $F_{(3,18)} = 1.817$, $P = 0.180$ ($n = 7$).

could those projections independently initiate relapse? After the extinction of VTA-NAcore, VTA-NAshell and VTA-IL-oICSS behavior, we excited these projections to induce reinstatement. Consistent with the above results, reinstatement behavior was significantly observed only when the VTA-NAcore DA projections were excited by 150 LSs at 80 Hz (Fig. 3a, active pokes: one-way RM ANOVA: laser priming main effect: $F_{(1,7)} = 8.784$, $P = 0.021$; inactive pokes: one-way RM ANOVA: laser priming main effect: $F_{(1,7)} = 0.943$, $P = 0.364$). *Post hoc* individual group comparisons assessed by Bonferroni tests revealed significant increases in the number of active pokes during laser-induced reinstatement compared to those during extinction, without a change in the number of inactive pokes. In contrast, the number of active pokes was not increased when the VTA-NAshell (Fig. 3b, active pokes: one-way RM ANOVA: laser priming main effect: $F_{(1,7)} = 3.653$, $P = 0.098$; inactive pokes: one-way RM ANOVA: laser priming main effect: $F_{(1,7)} = 4.020$, $P = 0.085$) and VTA-IL (Fig. 3c, active pokes: one-way RM ANOVA: laser priming main effect: $F_{(1,8)} = 2.617$, $P = 0.144$; inactive pokes: one-way RM ANOVA: laser priming main effect: $F_{(1,8)} = 2.445$, $P = 0.157$) projections were stimulated. The locations of implantation in the VTA, NAc and mPFC are schematically shown in Supplementary Fig. S5a–c. These results indicated that DA projections from the VTA to the NAcore could independently initiate reinstatement and were not innervated by other circuits.

Cocaine-associated cues activate VTA DA neurons during reinstatement

Next, we examined whether a similar DA mechanism underlies cue-induced reinstatement of cocaine-seeking behavior. After cocaine self-administration, the activity of VTA DA neurons was recorded during extinction and reinstatement (Fig. 4a). The expression of GCaMP6m on VTA DA neurons is shown in Fig. 4b, and the colocation of TH and GCaMP6m is shown in Supplementary Fig. S6a. In the behavior test, the cue induced significant reinstatement of cocaine-seeking behavior (Fig. 4c, active pokes: one-way RM ANOVA: cue priming main effect: $F_{(1,4)} = 18.878$, $P = 0.012$; inactive pokes: one-way RM ANOVA: cue priming main effect: $F_{(1,4)} = 0.0437$, $P = 0.845$). *Post hoc* individual group comparisons by Bonferroni tests revealed significant increases in the number of active pokes during laser-induced reinstatement compared to those during extinction, without a change in the number of inactive pokes. At the same time, the GCaMP6m signal was recorded to reflect the activity of VTA DA neurons during extinction and relapse tests. Fig. 4d shows representative heatmaps illustrating DA neuron activation (yellow) and depression (blue). Figure 4e shows the intracellular Ca^{2+} signal in VTA DA neurons during 5-s cue exposure, illustrating a significant increase in intracellular Ca^{2+} levels during reinstatement tests compared to those during extinction (absence of cue). Quantitative analysis of the averaged $\Delta F/F$ across the 5-s cue exposure revealed a significant increase in the activity of VTA DA neurons during cue-induced reinstatement compared to extinction (Fig. 4f, paired *t* test, $t = -2.552$, $P = 0.034$). The locations of implantation in the VTA are schematically shown in Supplementary Fig. S6b. The results showed that cue-induced reinstatement was accompanied by an increase in VTA DA neuron firing.

Chemogenetic inhibition of DA transmission in the NAcore blocks cue-induced reinstatement of cocaine-seeking behavior

To determine which specific DA projection pathways underlie cue-induced reinstatement of cocaine-seeking behavior, we used chemogenetic approaches to selectively inhibit DA transmission in the projection terminals in the NAcore, NAshell, PFC-IL or PFC-PL. Microinjections of CNO into the NAcore compared to microinjections of vehicle significantly decreased only cue-induced reinstatement of cocaine-seeking behavior (Fig. 5c, active pokes: one-way RM ANOVA, treatment main effect: $F_{(3,21)} = 16.434$, $P < 0.001$; inactive pokes, treatment main effect: $F_{(3,21)} = 1.929$, $P = 0.156$). In contrast, microinjections of CNO to any of the other projection areas (i.e., NAshell, PFC-IL, and PFC-PL) had no effects on cue-induced reinstatement of cocaine-seeking behavior (Fig. 5d, active pokes: one-way RM ANOVA, treatment main effect: $F_{(3,9)} = 3.055$, $P = 0.084$; inactive pokes: one-way RM ANOVA, treatment main effect: $F_{(3,9)} = 3.181$, $P = 0.078$. Figure 5e, active pokes: one-way RM ANOVA, treatment main effect: $F_{(3,6)} = 65.591$, $P < 0.001$; inactive pokes: one-way RM ANOVA, treatment main effect: $F_{(3,6)} = 0.667$, $P = 0.603$. Figure 5f, active pokes: one-way RM ANOVA, treatment main effect: $F_{(3,9)} = 21.690$, $P < 0.001$; inactive pokes: one-way RM ANOVA, treatment main effect: $F_{(3,9)} = 0.606$, $P = 0.628$). The locations of implantation in the NAc and mPFC are schematically shown in Supplementary Fig. S7a–d. These results indicated that the VTA-NAcore DA projection pathway was critical to cue-induced reinstatement of cocaine-seeking behavior.

Optogenetic activation of DA release in the NAcore triggers cue-induced cocaine seeking

Finally, we examined whether brief stimulation of DA release in the NAcore or other DA projection regions can trigger extinguished cocaine-seeking behavior (Fig. 6b). Notably, brief optical stimulation (100 laser pulses at 20 Hz) of DA terminals in the NAcore triggered the reinstatement of cocaine-seeking behavior (Fig. 6c, active pokes: one-way RM ANOVA on ranks: laser priming main effect: $P = 0.039$; inactive pokes: one-way RM ANOVA: laser priming main effect: $F_{(1,8)} = 0.151$, $P = 0.708$). In contrast, optogenetic stimulation (100 laser pulses at 20 or 80 Hz) of other DA projection regions failed to trigger the reinstatement of drug-seeking behavior in mice after the extinction of cocaine self-administration (Fig. 6d, VTA-NAshell, active poke: one-way RM ANOVA: laser priming main effect: $F_{(3,18)} = 1.239$, $P = 0.325$; inactive poke: one-way RM ANOVA: laser priming main effect: $F_{(3,18)} = 0.930$, $P = 0.446$. Figure 6e, VTA-IL: active poke: one-way RM ANOVA: laser priming main effect: $F_{(3,18)} = 0.696$, $P = 0.566$; inactive poke: one-way RM ANOVA: laser priming main effect: $F_{(3,18)} = 1.177$, $P = 0.346$. Figure 6f, VTA-PL: active poke: one-way RM ANOVA: laser priming main effect: $F_{(3,21)} = 0.621$, $P = 0.609$; inactive poke: one-way RM ANOVA: laser priming main effect: $F_{(3,21)} = 0.709$, $P = 0.557$). The locations of implantation in the NAc and mPFC are schematically shown in Supplementary Fig. S8a–d. These findings suggested that the activation of the VTA-NAcore DA projection pathway, but not other pathways, was sufficient to trigger the reinstatement of cocaine-seeking behavior.

DISCUSSION

In this study, we used two animal models, cue-induced reinstatement of oICSS and cue-induced reinstatement of cocaine-seeking behavior, to explore the role of DA in cue-induced relapse. There were two important findings. First, laser stimulation of VTA DA neurons or their projection terminals is rewarding. After extinction from oICSS, laser priming to briefly stimulate VTA DA neurons or their individual terminals reinstated the extinguished oICSS maintained by cues alone in mice previously trained to self-stimulate VTA DA neurons or each of the projection terminals. To the best of our knowledge, this is the first study to use this new oICSS animal model to study the neural mechanisms underlying cue-induced relapse. Second, we found that re-exposure of the mice to cocaine-associated cues (lights) reinstated extinguished cocaine-seeking behavior, accompanied by a significant increase in the intracellular GCaMP signal in VTA DA neurons. Importantly, optogenetic stimulation of DA projections in the NAcore, but not in the other DA projection regions, triggered the reinstatement of extinguished cocaine-seeking behavior, while chemogenetic inhibition of DA projections in the NAcore inhibited cue-induced reinstatement of cocaine-seeking behavior in DAT-Cre mice. Again, these findings, for the first time, indicated that cue-induced reinstatement of drug-seeking behavior was at least in part mediated by the activation of the VTA-NAcore projection pathway.

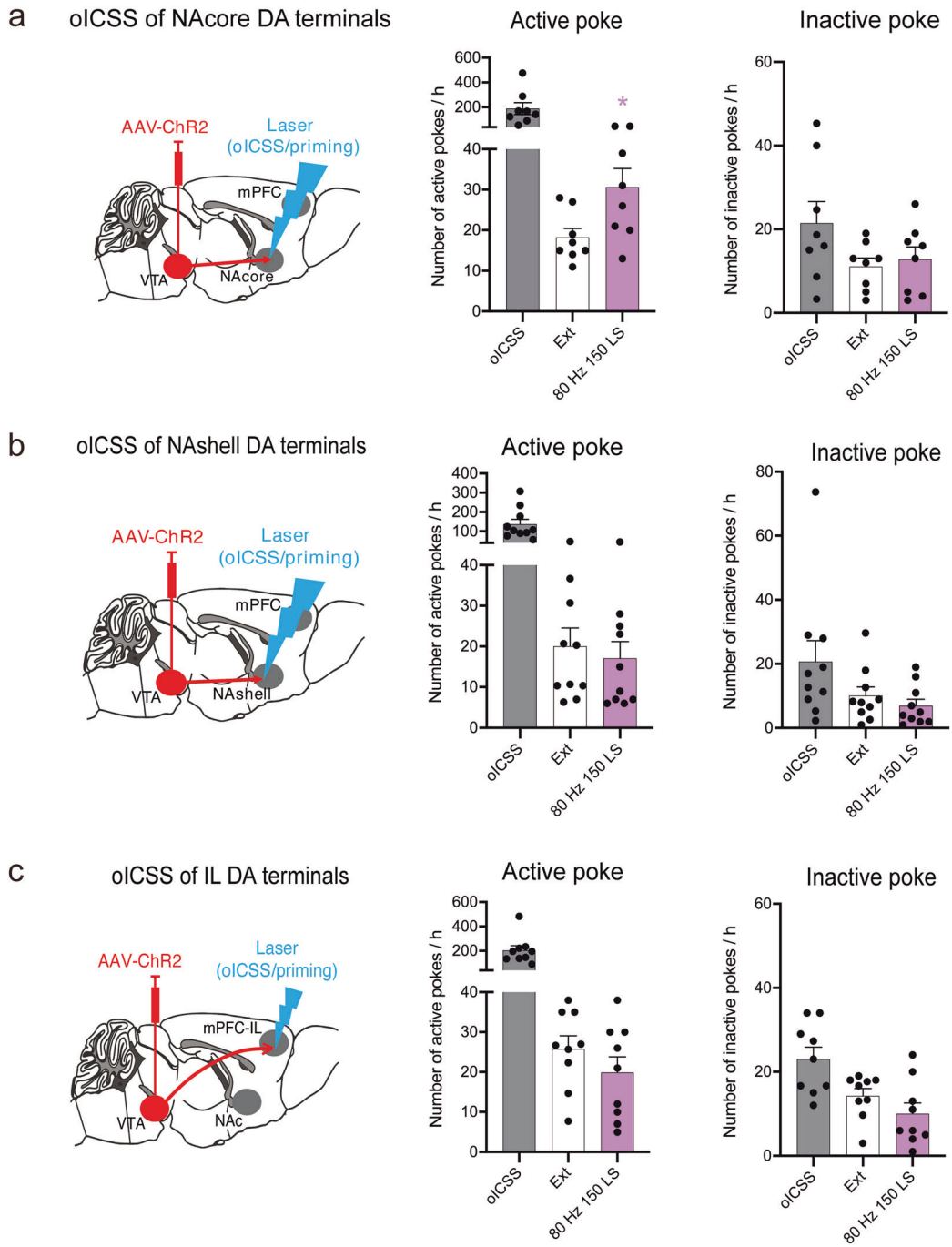

Fig. 3 VTA-NAcore DA projection pathway initiates brain-stimulation reward. a Mean numbers of nose pokes in the active and inactive holes during the last 3 sessions of the oICSS of VTA-NAcore DA projections, the last 3 sessions of extinction, and the laser-induced reinstatement test. The activation of VTA-NAcore DA projections (80-Hz, 150 laser pulses) reinstated active-poke responses in mice after the extinction of oICSS. One-way RM ANOVA revealed a laser priming main effect: $F_{(1,7)} = 8.784$, $P = 0.021$. *Post hoc* Bonferroni tests revealed that the activation of VTA-NAcore DA projections resulted in a statistically significant difference in reinstatement active-poke responses (*$P < 0.05$, compared to the mean of last 3 sessions of extinction, $n = 8$). **b** Mean numbers of nose pokes in active and inactive holes during the last 3 sessions of the oICSS of VTA-NAshell DA projections, the last 3 sessions of extinction, and the laser-induced reinstatement test. The activation of the VTA-NAshell DA projections did not reinstate active-poke responses in mice after the extinction of oICSS. One-way RM ANOVA revealed a laser priming main effect: $F_{(1,7)} = 3.653$, $P = 0.098$ ($n = 8$). **c** Mean numbers of nose pokes in the active and inactive holes during the last 3 sessions of the oICSS of VTA-IL DA projections, the last 3 sessions of extinction, and the laser-induced reinstatement test. The activation of the VTA-IL DA projection did not reinstate active-poke responses in mice after the extinction of oICSS. One-way RM ANOVA revealed a laser priming main effect: $F_{(1,8)} = 2.617$, $P = 0.144$ ($n = 9$).

It is generally believed that drug-associated cues can evoke intrinsic motivation and craving that leads to relapse. However, the role of DA in cue-induced reinstatement has largely been ignored, probably due to technical limitations in training mice to self-administer drugs of abuse and in detecting subtle cue-induced changes in DA release. Electrical ICSS (eICSS) is a commonly used behavioral procedure to study brain reward functions, and in this procedure, pressing a lever or nose poking

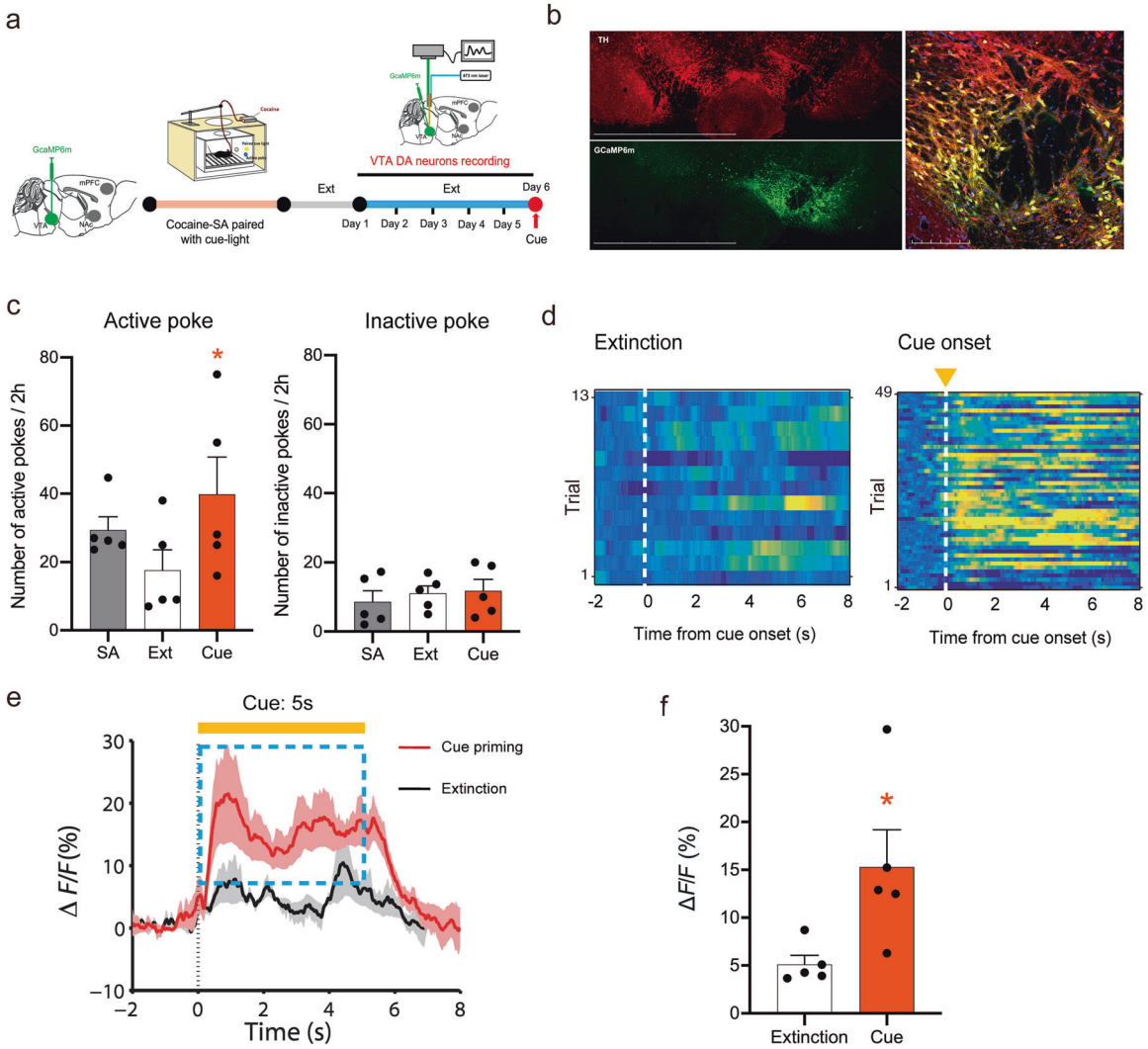

Fig. 4 Re-exposure to cocaine-associated cues activates VTA DA neurons. a Schedule of the fiber photometry of VTA DA neurons in cue-induced cocaine seeking. **b** Representative images illustrating GCaMP6m expression in the VTA in DAT-Cre mice after intra-VTA AAV-GCaMP6m microinjection. 10×, scale bar = 1500 μm; 20×, scale bar = 200 μm. **c** Mean numbers of nose pokes in active and inactive holes during the last 3 sessions of cocaine self-administration (SA), the last 3 sessions of extinction, and the cue reinstatement test. SA-associated cue lights reinstated active-poke responses in mice after the extinction of SA. One-way RM ANOVA revealed a cue priming main effect: $F_{(1,4)} = 18.878$, $P = 0.012$. *Post hoc* Bonferroni tests revealed that the differences in cue-induced active-poke responses were statistically significant ($^*P < 0.05$, compared to the last session of extinction, $n = 5$). Inactive pokes were not affected by cue light re-exposure after the extinction of SA. One-way RM ANOVA revealed a cue priming main effect: $F_{(1,4)} = 0.0437$, $P = 0.845$, $n = 5$. **d** The $\Delta F/F$ in cue priming and extinction are presented as heatmaps. Activation is presented in yellow, and depression is presented in blue. **e** The mean $\Delta F/F$ during the presence and absence of the cue (5 s) in extinction. The mean $\Delta F/F$ significantly increased during cue priming compared to the control condition in extinction, assessed by a paired *t* test, $t = -2.552$, $^*P < 0.05$. **f** Quantification of the activity of VTA DA neurons ($\Delta F/F$) in extinction and cue priming.

results in the delivery of brief electrical pulses to a discrete brain region via an implanted electrode [34, 35]. Using this model, it was well documented that the stimulation of the medial forebrain bundle (MFB) is rewarding [36–38], while eICSS has not been used to study the reinstatement of reward-seeking behavior. Compared to eICSS, oICSS has several obvious advantages, including a more robust lever response, neural substrate specificity and fewer unwanted side effects [39, 40]. Combining these advantages of oICSS with the multiple types of transgenic mice available, we further explored the possible utility of this procedure to study the neural mechanisms underlying drug- or cue-induced reinstatement of reward-seeking behavior. Our findings are similar to the recent finding with oICSS that the mesolimbic DA was closely associated with Pavlovian conditioning or cue-conditioned secondary reward [28, 41, 42]. In Pavlovian conditioning experiments, the activity in DA neurons turned discrete sensory cues into conditioned stimuli that elicited conditioned behaviors, including approaching the cue light and readily pressing a lever to receive conditioned cue presentations in the absence of laser activation [28]. However, both cue-conditioned reward and cue-induced reinstatement display similar behavioral responses (pressing a lever or nose poking a hole), and the neurobiological mechanisms underlying cue-conditioned reward and reinstatement response are significantly different. The former reflects the reinforcing process, which maintains reward-taking behavior (i.e., compulsive drug use in addiction), while the latter is involved in enduring neuroadaptations that occur during extinction and reinstatement, which is more complicated and involves emotions

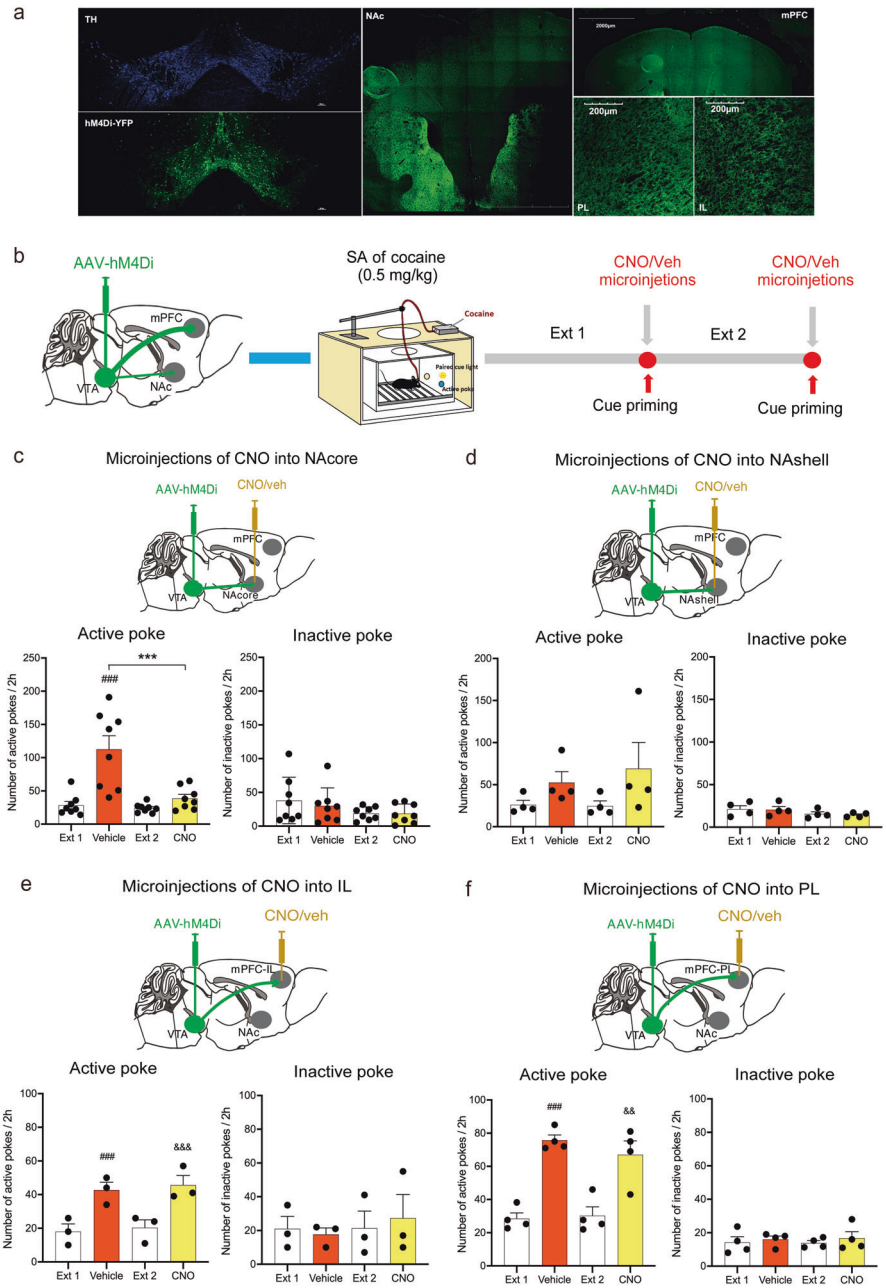

Fig. 5 Chemogenetic inactivation of the VTA-NAcore pathway selectively blocks cue-induced reinstatement of cocaine-seeking behavior. **a** Representative images illustrating hM4Di-mCherry expression in the VTA, NAc and mPFC in DAT-Cre mice. 10×, scale bar = 2000 μm; 20×, scale bar = 200 μm. **b** Schematic schedule of the experiments conducted. **c** Microinjection of CNO into the NAcore significantly decreased the cue-induced active-poke responses after the extinction of cocaine self-administration (SA). One-way RM ANOVA: treatment main effect: $F_{(3,21)} = 16.434$, $P < 0.001$. *Post hoc* Bonferroni tests revealed that the differences in cue-induced active-poke responses were statistically significant ($^{###}P < 0.001$, compared to the mean of the last 3 sessions of Ext 1), and the differences in cue-induced active-poke responses during CNO or vehicle microinjection were significantly different ($^{***}P < 0.01$, compared to vehicle, $n = 8$). **d** Microinjection of CNO into the NAshell had no effects on cue-induced active-poke responses in mice. One-way RM ANOVA: treatment main effect: $F_{(3,9)} = 3.055$, $P = 0.084$ ($n = 4$). **e** Microinjection of CNO into the IL had no effects on cue-induced active-poke responses in mice. One-way RM ANOVA: treatment main effect: $F_{(3,6)} = 65.591$, $P < 0.001$. *Post hoc* Bonferroni tests revealed that the differences in cue-induced active-poke responses following vehicle administration were statistically significant ($^{###}P < 0.001$, compared to Ext 1), differences in cue-induced active-poke responses following CNO administration were significant ($^{&&&}P < 0.001$, compared to the mean of the last 3 sessions of Ext 2), and differences between CNO and vehicle microinjections were not significantly different ($P > 0.05$, compared to vehicle, $n = 3$). **f** Microinjection of CNO into the PL had no effects on cue-induced active-poke responses in mice. One-way RM ANOVA: treatment main effect: $F_{(3,9)} = 21.690$, $P < 0.001$. *Post hoc* Bonferroni tests revealed that differences in the cue-induced active-poke responses during vehicle administration were statistically significant ($^{###}P < 0.001$, compared to Ext 1), differences in the cue-induced active-poke responses during CNO were significant ($^{&&}P < 0.01$, compared to the mean of the last 3 sessions of Ext 2), and the differences between CNO and vehicle microinjections were not significantly different ($P > 0.05$, compared to vehicle, $n = 4$).

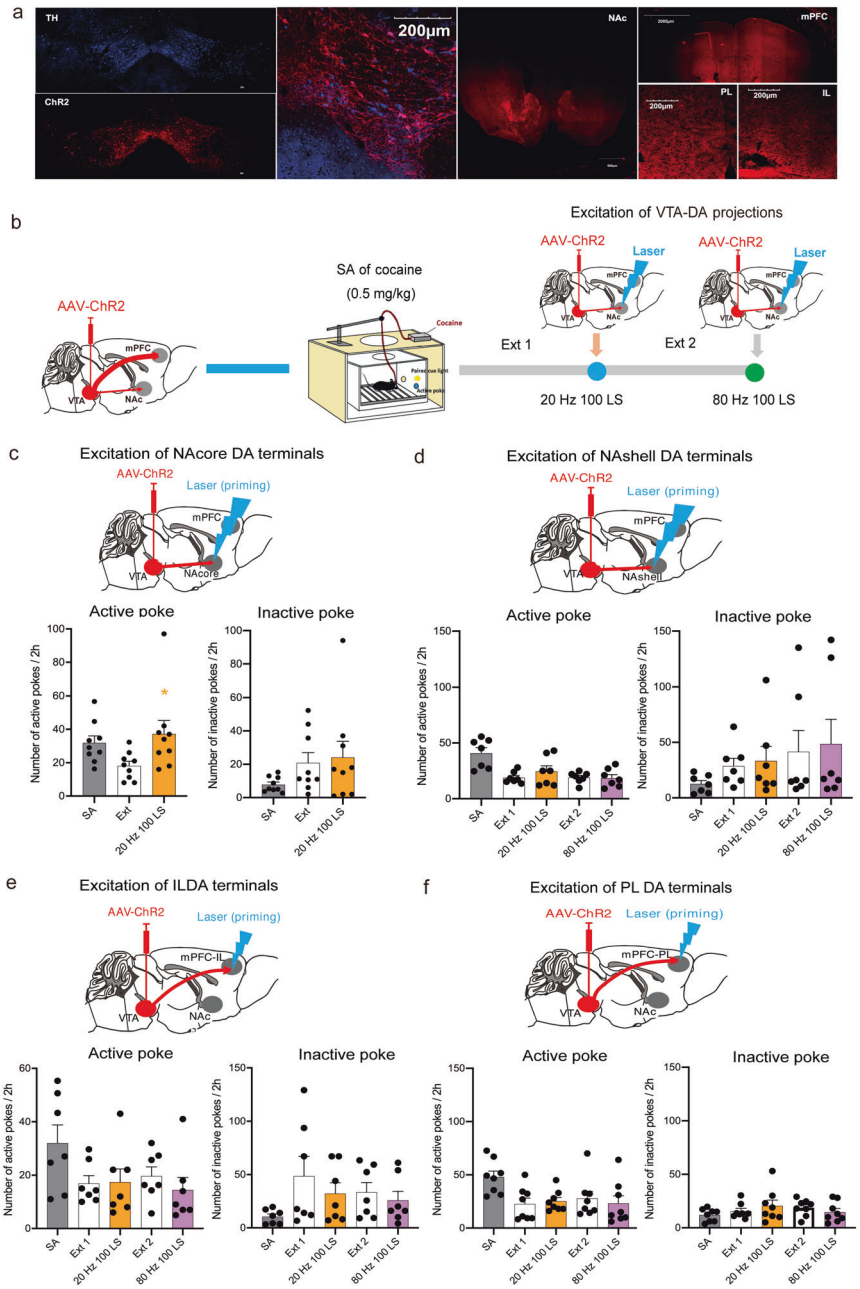

Fig. 6 Optical activation of the VTA-NAcore DA projection pathway selectively reinstates extinguished cocaine-seeking behavior. **a** Representative images illustrating ChR2-mCherry expression in the VTA, NAc and mPFC in DAT-Cre mice after intra-VTA AAV-ChR2 microinjection. 10×, scale bar = 2000 μm; 20×, scale bar = 200 μm. **b** Schematic schedule of experiments: after the extinction of cocaine self-administration (SA), a laser was used to activate DA projections to induce cocaine relapse. **c** Mean numbers of nose pokes in active and inactive holes during the last 3 sessions of SA, the last 3 sessions of extinction, and the laser-induced reinstatement test. The activation of VTA-NAcore DA projections (20-Hz, 100 laser pulses) reinstated active-poke responses in mice after the extinction of SA. One-way RM ANOVA on ranks revealed a laser priming main effect: $P = 0.039$. *Post hoc* Tukey's test revealed that activation of VTA-NAcore DA projections resulted in a difference in reinstated active-poke responses that was statistically significant (*$P < 0.05$, compared to the mean of last 3 sessions of extinction, $n = 9$). Inactive pokes were not affected by laser priming after the extinction of SA. One-way RM ANOVA revealed a treatment main effect: $F_{(1,8)} = 0.151$, $P = 0.708$. **d** Activation of DA projections to the NAshell did not reinstate active-poke responses in mice after the extinction of SA. One-way RM ANOVA revealed a laser priming main effect: $F_{(3,18)} = 1.239$, $P = 0.325$, $n = 7$. **e** Activation of DA projections to the IL did not reinstate active-poke responses in mice after the extinction of SA. One-way RM ANOVA revealed a laser priming main effect: $F_{(3,18)} = 0.696$, $P = 0.566$, $n = 7$. **f** Activation of DA projections to the PL did not reinstate active-poke responses in mice after the extinction of SA. One-way RM ANOVA revealed a laser priming main effect: $F_{(3,21)} = 0.621$, $P = 0.609$, $n = 8$.

and incentive motivation. There is a profound increase in the motivation to resume drug-seeking behavior in abstinent subjects during extinction in drug-associated contexts [43, 44]. Based on our studies, we demonstrated that optical stimulation of DA neurons in the VTA or their terminals in the NAcore, NAshell, or mPFC-IL was sufficient in maintaining oICSS, while optical stimulation of DA neurons in only the NAcore was sufficient and necessary for cue-induced reinstatement since re-exposure to reward-associated cues can activate VTA DA neurons. Thus, oICSS in DAT-Cre mice may be used as a new animal model to study the

neural mechanisms underlying cue-induced relapse. In contrast to DA projections to the NAcore, we did not find evidence supporting an important role of DA projections to the mPFC in cue-induced reinstatement in the oICSS models.

As mentioned above, DA projections to the NAcore have been shown to be involved in the motivation to seek and take drugs. Previous studies showed that the blockade of DA D1 or D2 receptors in the NAcore attenuated cue-evoked cocaine- or heroin-seeking behavior [12, 28], and the activation of D2-MSNs or increased DA release in the NAc has been associated with increased motivation to seek drugs [14]. The D1 receptor in the NAshell has been shown to be involved in context-induced relapse [12]. It was reported that optogenetic inhibition of VTA-NAcore projections decreased the relapse induced by exposure to cocaine-plus-cue [45]. Since cocaine is a potent DA enhancer that blocks the dopamine transporter (DAT), it is reasonable to believe that the mesolimbic DA system is activated mainly by cocaine priming. Thus, the inhibition of DA transmission in the NAcore attenuates the cocaine-primed reinstatement response. However, it is unknown whether cocaine-associated cues alone (in the absence of cocaine) can also activate the same pathway and therefore underlie cue-induced relapse. To address this question, we carried out a series of experiments using optogenetic, chemogenetic and transgenic approaches in this study. We found that the re-exposure of mice to cocaine-associated cues (lights) reinstated extinguished cocaine-seeking behavior, accompanied by a significant increase in the intracellular GCaMP signal in VTA DA neurons. Although the results were similar to those of previous studies with electrical technology [46, 47], the fiber photometry experiment in the present study was more specialized and precise to record DA activity in the VTA in freely moving and behaving animals. In previous research, Jiang's study used conditioned place preference models and tested whether the firing of VTA neurons significantly changed when CPP was reinstated through electrophysiology methods [46]. The lack of neural specificity is the most important problem. Another study recorded the activity of VTA DA neurons with GCaMP tools when mice relapsed to alcohol induced by context [48]. Our results indicated that DA neurons were excited when the cue induced cocaine relapse. This finding may provide new evidence for the role of VTA DA neurons, especially in cue-induced reinstatement, in cocaine self-administration. We also found that optogenetic stimulation of the VTA-NAcore pathway, but not the other pathways, reinstated extinguished cocaine-seeking behavior, and chemogenetic inhibition of the VTA-NAcore DA pathway attenuated reinstatement in response to cocaine-associated cues, consistent with the findings of the above research in oICSS. These results suggested that DA is not only a modulator of reward but also a primary trigger in cue-induced relapse. This finding of DA projections from the VTA to the NAcore was similar to Mahler's research on cocaine addiction and Liu's research on alcohol addiction [48, 49]. Although different activation methods were used, including chemical genetics in Mahler's study and optogenetics in our experiment, both of the studies showed that DA specifically stimulated the DA projections to the NAcore to induce the reinstatement of cocaine SA without cues present. Moreover, our study further demonstrated that the pathway was necessary in cue-induced reinstatement with the chemogenetic inhibition approach. Although several DA neurons in the VTA corelease glutamate, VTA neurons expressing the type-2 vesicular glutamate transporter (VGLUT2) are few (~36%) [50]. In addition, electrophysiological data demonstrated that VTA neurons releasing glutamate mainly project to the NAshell, not the NAcore [51, 52]. In addition, we prefered to emphasize the importance of NAcore-projecting DA neurons in cue-induced relapse but not only DA neurotransmitter. Generally, the phenomenon of VTA DA neuron Glu corelease may have little effect on our conclusion.

Nonetheless, the DA pathway projecting from the VTA to the mPFC did show significant effects on cue-induced reinstatement in both oICSS and cocaine-induced SA models. These findings were similar to those from Mahler's research, only the stimulation of DA projections to the mPFC was insufficient to induce reinstatement without the presence of cues. However, this result seemed to be inconsistent with that of previous research; increasing DA efflux in the mPFC may be associated with cue-induced reinstatement of methamphetamine-seeking behavior [15], and similarly, microinfusions of cocaine into the mPFC-PL can reinstate cocaine-seeking behavior [53]. However, these results still cannot explain whether the DA pathway of the VTA-mPFC plays a direct or indirect role in the reinstatement process. It was reported that the inactivation of glutamatergic neurons in the IL initiated cocaine-seeking behavior [54–56], suggesting an important role of glutamate in the mPFC-IL in cocaine reinstatement. Thus, the DA circuits of the VTA-mPFC in cue-induced reinstatement in addiction are still worth in-depth study.

In conclusion, in the present study, we found that DA neurons in the VTA can be activated by re-exposure to drug-associated cues, which may trigger cue-induced relapse. Furthermore, the mesolimbic DA projections from the VTA to the NAcore, and not to the other brain regions (NAshell or mPFC), appear to be critical in cue-induced relapse to drug- or reward-seeking behavior. These new findings not only provide new insights into the neurobiology of drug reward and relapse but also identify new targets for medication development related to relapse prevention. The lack of an investigation of the activity of VTA DA neurons projecting to the NAcore, NAshell and IL during cue-induced relapse is a shortcoming of the present study, and we will investigate this activity in future studies.

ACKNOWLEDGEMENTS

This work was supported by the National Natural Science Foundation of China (81573405 and U1502225), Natural Science Foundation of Beijing (7212159), National Key R&D Program of China (2016YFC0800907), National Key R&D Program of China (2017YFC131040), Medical Innovation Program (16CXZ033) and Beijing Nova Program (xx2014A014).

AUTHOR CONTRIBUTIONS

RS, NW and JL initiated this project. RS designed the study. TYZ and XH bred the mice. MYJ and XYD conducted the experiments and analyzed the data. MML provided technical support. MYJ and RS wrote and revised the manuscript.

ADDITIONAL INFORMATION

Supplementary information The online version contains supplementary material available at https://doi.org/10.1038/s41401-022-00866-x.

Competing interests: The authors declare no competing interests.

REFERENCES

1. Kenny PJ, Hoyer D, Koob GF. Animal models of addiction and neuropsychiatric disorders and their role in drug discovery: honoring the legacy of Athina Markou. Biol Psychiatry. 2018;83:940–6.
2. Sinha R, Jastreboff AM. Stress as a common risk factor for obesity and addiction. Biol Psychiatry. 2013;73:827–35.
3. Wolf ME. Synaptic mechanisms underlying persistent cocaine craving. Nat Rev Neurosci. 2016;17:351–65.
4. See RE. Neural substrates of conditioned-cued relapse to drug-seeking behavior. Pharmacol Biochem Behav. 2002;71:517–29.
5. Wilson SJ, Sayette MA, Fiez JA. Prefrontal responses to drug cues: a neurocognitive analysis. Nat Neurosci. 2004;7:211–4.
6. Namba MD, Tomek SE, Olive MF, Beckmann JS, Gipson CD. The winding road to relapse: forging a new understanding of cue-induced reinstatement models and their associated neural mechanisms. Front Behav Neurosci. 2018;12:17.
7. Luscher C. Drug-evoked synaptic plasticity causing addictive behavior. J Neurosci. 2013;33:17641–6.
8. van Huijstee AN, Mansvelder HD. Glutamatergic synaptic plasticity in the mesocorticolimbic system in addiction. Front Cell Neurosci. 2014;8:466.

9. Maskos U, Molles BE, Pons S, Besson M, Guiard BP, Guilloux JP, et al. Nicotine reinforcement and cognition restored by targeted expression of nicotinic receptors. Nature. 2005;436:103–7.
10. Tan KR, Brown M, Labouebe G, Yvon C, Creton C, Fritschy JM, et al. Neural bases for addictive properties of benzodiazepines. Nature. 2010;463:769–74.
11. Williams JM, Galli A. The dopamine transporter: a vigilant border control for psychostimulant action. Handb Exp Pharmacol. 2006;175:215–32.
12. Bossert JM, Poles GC, Wihbey KA, Koya E, Shaham Y. Differential effects of blockade of dopamine D1-family receptors in nucleus accumbens core or shell on reinstatement of heroin seeking induced by contextual and discrete cues. J Neurosci. 2007;27:12655–63.
13. Saunders BT, Yager LM, Robinson TE. Cue-evoked cocaine "craving": role of dopamine in the accumbens core. J Neurosci. 2013;33:13989–4000.
14. Gallo EF, Meszaros J, Sherman JD, Chohan MO, Teboul E, Choi CS, et al. Accumbens dopamine D2 receptors increase motivation by decreasing inhibitory transmission to the ventral pallidum. Nat Commun. 2018;9:1086.
15. Parsegian A, See RE. Dysregulation of dopamine and glutamate release in the prefrontal cortex and nucleus accumbens following methamphetamine self-administration and during reinstatement in rats. Neuropsychopharmacology. 2014;39:811–22.
16. Spencer S, Garcia-Keller C, Roberts-Wolfe D, Heinsbroek JA, Mulvaney M, Sorrell A, et al. Cocaine use reverses striatal plasticity produced during cocaine seeking. Biol Psychiatry. 2017;81:616–24.
17. Russo SJ, Dietz DM, Dumitriu D, Morrison JH, Malenka RC, Nestler EJ. The addicted synapse: mechanisms of synaptic and structural plasticity in nucleus accumbens. Trends Neurosci. 2010;33:267–76.
18. Stefanik MT, Kupchik YM, Kalivas PW. Optogenetic inhibition of cortical afferents in the nucleus accumbens simultaneously prevents cue-induced transient synaptic potentiation and cocaine-seeking behavior. Brain Struct Funct. 2016;221:1681–9.
19. Wolf ME, Ferrario CR. AMPA receptor plasticity in the nucleus accumbens after repeated exposure to cocaine. Neurosci Biobehav Rev. 2010;35:185–211.
20. Gipson CD, Kupchik YM, Shen H, Reissner KJ, Thomas CA, Kalivas PW. Relapse induced by cues predicting cocaine depends on rapid, transient synaptic potentiation. Neuron. 2013;77:867–72.
21. Gipson CD, Reissner KJ, Kupchik YM, Smith AC, Stankeviciute N, Hensley-Simon ME, et al. Reinstatement of nicotine seeking is mediated by glutamatergic plasticity. Proc Natl Acad Sci USA. 2013;110:9124–9.
22. Shen H, Moussawi K, Zhou W, Toda S, Kalivas PW. Heroin relapse requires long-term potentiation-like plasticity mediated by NMDA2b-containing receptors. Proc Natl Acad Sci USA. 2011;108:19407–12.
23. Smith AC, Kupchik YM, Scofield MD, Gipson CD, Wiggins A, Thomas CA, et al. Synaptic plasticity mediating cocaine relapse requires matrix metalloproteinases. Nat Neurosci. 2014;17:1655–7.
24. Gunaydin LA, Grosenick L, Finkelstein JC, Kauvar IV, Fenno LE, Adhikari A, et al. Natural neural projection dynamics underlying social behavior. Cell. 2014;157:1535–51.
25. Kennedy RT. Emerging trends in in vivo neurochemical monitoring by microdialysis. Curr Opin Chem Biol. 2013;17:860–7.
26. Perry M, Li Q, Kennedy RT. Review of recent advances in analytical techniques for the determination of neurotransmitters. Anal Chim Acta. 2009;653:1–22.
27. Adamantidis AR, Tsai HC, Boutrel B, Zhang F, Stuber GD, Budygin EA, et al. Optogenetic interrogation of dopaminergic modulation of the multiple phases of reward-seeking behavior. J Neurosci. 2011;31:10829–35.
28. Saunders BT, Richard JM, Margolis EB, Janak PH. Dopamine neurons create Pavlovian conditioned stimuli with circuit-defined motivational properties. Nat Neurosci. 2018;21:1072–83.
29. Tsai HC, Zhang F, Adamantidis A, Stuber GD, Bonci A, de Lecea L, et al. Phasic firing in dopaminergic neurons is sufficient for behavioral conditioning. Science. 2009;324:1080–4.
30. Lammel S, Lim BK, Malenka RC. Reward and aversion in a heterogeneous midbrain dopamine system. Neuropharmacology. 2014;76:351–9.
31. Wang XF, Liu JJ, Xia J, Liu J, Mirabella V, Pang ZP. Endogenous glucagon-like peptide-1 suppresses high-fat food intake by reducing synaptic drive onto mesolimbic dopamine neurons. Cell Rep. 2015;12:726–33.
32. Han X, Jing MY, Zhao TY, Wu N, Song R, Li J. Role of dopamine projections from ventral tegmental area to nucleus accumbens and medial prefrontal cortex in reinforcement behaviors assessed using optogenetic manipulation. Metab Brain Dis. 2017;32:1491–502.
33. Song R, Zhang HY, Li X, Bi GH, Gardner EL, Xi ZX. Increased vulnerability to cocaine in mice lacking dopamine D3 receptors. Proc Natl Acad Sci USA. 2012;109:17675–80.
34. Moerke MJ, Negus SS. Role of agonist efficacy in exposure-induced enhancement of mu opioid reward in rats. Neuropharmacology. 2019;151:180–8.
35. Negus SS, Miller LL. Intracranial self-stimulation to evaluate abuse potential of drugs. Pharmacol Rev. 2014;66:869–917.
36. Wise RA. Addictive drugs and brain stimulation reward. Annu Rev Neurosci. 1996;19:319–40.
37. German DC, Holloway FA. Directionality of rewarding impulses within the medial forebrain bundle self-stimulation system of the rat. Science. 1973;179:1345–7.
38. Huguet G, Kadar E, Serrano N, Tapias-Espinosa C, Garcia-Brito S, Morgado-Bernal I, et al. Rewarding deep brain stimulation at the medial forebrain bundle favours avoidance conditioned response in a remote memory test, hinders extinction and increases neurogenesis. Behav Brain Res. 2020;378:112308.
39. Mylius J, Happel MF, Gorkin AG, Huang Y, Scheich H, Brosch M. Fast transmission from the dopaminergic ventral midbrain to the sensory cortex of awake primates. Brain Struct Funct. 2015;220:3273–94.
40. Weidner TC, Vincenz D, Brocka M, Tegtmeier J, Oelschlegel AM, Ohl FW, et al. Matching stimulation paradigms resolve apparent differences between optogenetic and electrical VTA stimulation. Brain Stimul. 2020;13:363–71.
41. Flagel SB, Clark JJ, Robinson TE, Mayo L, Czuj A, Willuhn I, et al. A selective role for dopamine in stimulus-reward learning. Nature. 2011;469:53–7.
42. Saunders BT, Robinson TE. The role of dopamine in the accumbens core in the expression of Pavlovian-conditioned responses. Eur J Neurosci. 2012;36:2521–32.
43. Grimm JW, Hope BT, Wise RA, Shaham Y. Neuroadaptation. Incubation of cocaine craving after withdrawal. Nature. 2001;412:141–2.
44. Pickens CL, Airavaara M, Theberge F, Fanous S, Hope BT, Shaham Y. Neurobiology of the incubation of drug craving. Trends Neurosci. 2011;34:411–20.
45. Stefanik MT, Kupchik YM, Brown RM, Kalivas PW. Optogenetic evidence that pallidal projections, not nigral projections, from the nucleus accumbens core are necessary for reinstating cocaine seeking. J Neurosci. 2013;33:13654–62.
46. Jiang JX, Liu H, Huang ZZ, Cui Y, Zhang XQ, Zhang XL, et al. The role of CA3-LS-VTA loop in the formation of conditioned place preference induced by context-associated reward memory for morphine. Addict Biol. 2018;23:41–54.
47. Nishino H, Ono T, Muramoto K, Fukuda M, Sasaki K. Neuronal activity in the ventral tegmental area (VTA) during motivated bar press feeding in the monkey. Brain Res. 1987;413:302–13.
48. Liu Y, Jean-Richard-Dit-Bressel P, Yau JO, Willing A, Prasad AA, Power JM, et al. The mesolimbic dopamine activity signatures of relapse to alcohol-seeking. J Neurosci. 2020;40:6409–27.
49. Mahler SV, Brodnik ZD, Cox BM, Buchta WC, Bentzley BS, Quintanilla J, et al. Chemogenetic manipulations of ventral tegmental area dopamine neurons reveal multifaceted roles in cocaine abuse. J Neurosci. 2019;39:503–18.
50. Yamaguchi T, Wang HL, Li X, Ng TH, Morales M. Mesocorticolimbic glutamatergic pathway. J Neurosci. 2011;31:8476–90.
51. Mingote S, Amsellem A, Kempf A, Rayport S, Chuhma N. Dopamine-glutamate neuron projections to the nucleus accumbens medial shell and behavioral switching. Neurochem Int. 2019;129:104482.
52. Yoo JH, Zell V, Gutierrez-Reed N, Wu J, Ressler R, Shenasa MA, et al. Ventral tegmental area glutamate neurons co-release GABA and promote positive reinforcement. Nat Commun. 2016;7:13697.
53. Park WK, Bari AA, Jey AR, Anderson SM, Spealman RD, Rowlett JK, et al. Cocaine administered into the medial prefrontal cortex reinstates cocaine-seeking behavior by increasing AMPA receptor-mediated glutamate transmission in the nucleus accumbens. J Neurosci. 2002;22:2916–25.
54. LaLumiere RT, Niehoff KE, Kalivas PW. The infralimbic cortex regulates the consolidation of extinction after cocaine self-administration. Learn Mem. 2010;17:168–75.
55. LaLumiere RT, Smith KC, Kalivas PW. Neural circuit competition in cocaine-seeking: roles of the infralimbic cortex and nucleus accumbens shell. Eur J Neurosci. 2012;35:614–22.
56. Peters J, LaLumiere RT, Kalivas PW. Infralimbic prefrontal cortex is responsible for inhibiting cocaine seeking in extinguished rats. J Neurosci. 2008;28:6046–53.